Photoenhanced uptake of gaseous NO2 on solid organic compounds: a photochemical source of HONO?

C. George, Rafal Strekowski, J. Kleffmann, K. Stemmler, M. Ammann

Photoenhanced Uptake of Gaseous NO_2 on Solid Organic Compounds: A photochemical source of HONO

C George [a]*, R S Strekowski [a(#)], J Kleffmann [b], K Stemmler [c] and M Ammann [c]

[a] *Laboratoire d'Application de la Chimie à l 'Environnement (UCBL-CNRS) 43 boulevard du 11 Novembre 1918, F-69622 Villeurbanne, France. Fax:+33 (0)4 72 44 8114; Tel: +33 (0)4 72 43 1489, E-mail: christian.george@univ-lyon1.fr*

[b] *Physikalische Chemie/FB C, Bergische Universität Wuppertal, 42097 Wuppertal, Germany. Fax:+49 202 439 2505; Tel: +49 202 439 3534, E-mail: kleffman@uni-wuppertal.de*

[c] *Labor für Radio- und Umweltchemie, Paul Scherrer Institut, 5232 Villigen, Switzerland. Fax:+41 56 310 4435; Tel: +41 56 310 4049, E-mail: markus.ammann@psi.ch;konrad.stemmler@psi.ch.*

***This submission was created using the RSC Article Template* (*DO NOT DELETE THIS TEXT*)**
(*LINE INCLUDED FOR SPACING ONLY - DO NOT DELETE THIS TEXT*)

In several recent field campaigns the existence of a strong daytime source of nitrous acid was demonstrated. The mechanism of this source remains unclear. Accordingly, in the present laboratory study, the effect of light (in the range 300-500nm) on the uptake kinetics of NO_2 on various surfaces taken as proxies for organic surfaces encountered in the troposphere (as organic aerosol but also ground surfaces) was investigated. In this collaborative study, the uptake kinetics and product formation rate were measured by different flow tube reactors in combination with a sensitive HONO instrument. Uptake on phenolic species was significantly enhanced when irradiated with light of 300 – 420 nm, and HONO was formed with high yield when the gas was humidified. Adding a stronger absorber, such as BBA, further enhanced the reactivity of the substrate. Based on the results reported a mechanism is suggested, in which photosensitised electron transfer are occurring. The results show that HONO can be efficiently formed during the day in the atmosphere at much longer wavelengths compared to the recently proposed nitrate photolysis.

Introduction

Since the initial detection of nitrous acid (HONO) in the atmosphere by Perner and Platt [1], many studies have shown that nitrous acid may accumulate during night-time before undergoing photolysis in the early morning:

$$HONO + h\nu \rightarrow NO + OH \quad (1),$$

which creates an important morning OH radical burst [2,3]. In recent studies[4-9], a significant contribution of the HONO photolysis to the integrated OH yield of up to 60 % was calculated.. As both products of reaction (1) are key players in the processes leading to photochemical pollution, it is essential to understand and identify all sources of tropospheric nitrous acid.

Despite many studies, to date the formation mechanism of HONO in the atmosphere is still not completely understood. It appears that all gas phase reactions are too slow to explain night-time HONO formation [10]. In addition, direct emissions can only partly explain atmospheric HONO levels [9,11]. Accordingly, different heterogeneous formation pathways have been postulated. For example, it has been suggested that HONO is formed by the heterogeneous conversion of nitrogen dioxide (NO_2) on soot surfaces [12,13]. However, recent studies demonstrated that this non-catalytic reaction cannot explain current HONO levels in the atmosphere [14,15]. Based on correlation studies, it was proposed that the heterogeneous reaction of NO and NO_2 on particle surfaces is a significant atmospheric HONO source [10]. However, field studies [16] and a laboratory investigation in which the reaction was studied under humidity levels and NO_x concentrations prevailing in the atmosphere [17] indicate that this reaction is unimportant. Laboratory studies have also proposed that the reaction of NO with adsorbed nitric acid (HNO_3) represents a potential HONO source [18], however, a recent study which was performed at atmospheric humidity levels and NO_y concentrations much lower than the ones used in all other studies, demonstrates that this reaction is too slow to be of importance in the atmosphere [19].

Although it is commonly proposed that HONO is mainly formed by heterogeneous processes during the night, i.e. by the conversion of NO_2 on humid surfaces [20], the exact mechanism of the NO_2 conversion is still under discussion and remains unclear. In most studies, the following heterogeneous reaction was postulated [21]:

$$2\ NO_2 + H_2O \rightarrow HONO + HNO_3 \quad (2)$$

On the other hand, in a recent study, the reaction of NO_2 with organics dissolved in aqueous solutions was proposed [22]. In an aqueous solution, NO_2 may undergo electron transfer reactions with phenoxide ions, which have been previously investigated for methylphenols and hydroxybenzenes [23,24], catechins [25] and hydroxycinnamic acid derivatives [26]. The most important reactant is the deprotonated species, the phenoxide ion, leading to strongly pH dependent overall kinetics. The primary reaction product is the corresponding phenoxy type radical and nitrite ion or HONO [24]. A similar mechanism was shown to occur on solid 1,2,10-trihydroxyanthracene, where HONO has been observed as a primary product [27]. The kinetics seem to be driven by the presence of adsorbed water associated with this sparingly soluble compound, and the reaction rates remain relatively low, possibly due to the very small tendency of this weak acid to form the phenoxide ion under the experimental conditions employed.

These phenolic compounds are ubiquitously present in the environment. Hydroxybenzenes may be formed as intermediates in the photooxidation of aromatic compounds in the gas phase [28,29]. A variety of guaiacols, catechols and syringols are formed during combustion of biomass, mainly from lignin pyrolysis [30,31]. Furthermore, the microbial decomposition of vegetation leads to a large number of polyphenols along with their acid and aldehyde derivatives at significant conentrations in the soil [32].

The significance of the (dark) chemistry of NO_2 with these organic compounds in a polluted atmospheric aerosol heavily

depends on the total amount of aromatics appearing in the aqueous phase and on aerosol pH [33] and might be important in a biomass burning plume [34]. The significance in an aqueous or non-aqueous environment with a high content of these species combined with the presence of neutralizing minerals or organic acids, such as above soils, still needs to be investigated.

While the night time formation of HONO in the atmosphere may be reasonably well explained by direct emissions and heterogeneous conversion of NO_2 on ground surfaces with the different mechanisms mentioned above, measured concentrations significantly exceeded modelled values during the day [9]. Accordingly, a strong daytime source was postulated in recent studies to explain daytime concentrations of HONO over snow [e.g.35], ground and vegetation surfaces [5,36,37,9,38]. The source strength of this daytime source was estimated to be 200-1800 pptv/h [8,388] or to be ~20 times faster than all night-time sources of HONO [37]. The photolysis of nitrate and/or nitric acid on surfaces was postulated to explain these high daytime concentrations of HONO [5,38]. However, the exact mechanism of this photolytic HONO source still remains to be unanswered, e.g. the photolysis frequency of adsorbed HNO_3 was reported to be two orders of magnitude faster compared to the gas and the liquid phase, which is still unclear [38,39]. In addition, in a recent study in a large simulation chamber, the photolysis of HNO_3/nitrate was excluded to explain the observed photolytic HONO formation [40].

Therefore, we investigated the effect of light (in the range 300-500 nm) on the uptake kinetics of NO_2 on various surfaces taken as proxies for organic surfaces encountered in the troposphere. In this collaborative study, the uptake kinetics and product formation rates were measured using different flow tube reactors in combination with different analytical methods for NO_x and HONO detection. We will show that there is a substantial effect of light on the NO_2 uptake kinetics on organic surfaces and on the formation of nitrous acid.

Experimental

The heterogeneous interactions of gaseous NO_2 were studied on bulk surfaces by exposing different concentrations of gaseous NO_2 mixtures to selected solid organic films. The experimental approach is based on measuring the reactant gas concentration i.e., NO_2 gas, at the exit of a cylindrical flow reactor as a function of the distance (time) that the NO_2 gas is in contact with the solid organic surface. This flow tube method was used in two different configurations, one by coupling the reactor to a quadrupole mass spectrometer to detect NO_2 in the range of 10 to 100 ppm, and one by coupling a simpler version of the reactor to the LOPAP instrument and a chemiluminescence detector to detect HONO and NO_X in the lower ppb range.

a) Horizontal Coated Wall Reactor with MS Detection

The horizontal flow tube approach used in this study (see Figure 1) is similar to the one used in previous studies of heterogeneous reactions[41,42]. However, the horizontal reactor used in this work has been adapted with two UV lamps to study the effect of irradiation on the uptake of NO_2 gas on organic surfaces and the possible generation of nitrous acid (HONO). This point is discussed further in the section below.

A Pyrex tube with an internal volume of approximately 80 cm^3 and an inner diameter of 1.5 cm (S/V = 2.7 cm^{-1}) was used in all experiments. The cell was maintained at a constant temperature (±0.5 K) using a Huber CC130 thermostatically controlled bath by circulating a 1:1 ethanol+methanol mixture through the outer jacket. A Type J thermocouple (OMEGA Engineering, Inc.) with a stainless steel jacket was inserted into the reactor through a vacuum seal, allowing measurement of the temperature under precise experimental conditions employed. The geometry of the flow tube reactor was such that it allowed for the helium carrier

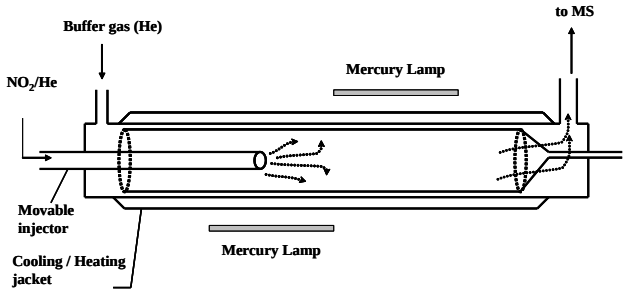

Figure 1. Schematic representation of the horizontal wall flow tube experimental approach used to measure the uptake of NO_2 on solid organic films.

and the reactant flows to enter at one end and the quadrupole mass spectrometer to be located downstream at the opposite end. All experiments were carried out at atmospheric pressure with the linear flow rate through the reactor in the range 3 to 10 cm s^{-1}. The flow tube was mounted horizontally and the organic layer was contained within the inner flow tube. In certain experiments, water vapour was added to the carrier He gas upstream to control the humidity. All experiments were performed under atmospheric pressure and the temperature range was T=278 K to 308 K. The reactant NO_2 gas was introduced into the reactor via a 0.635 cm o.d. and 50 cm long movable, Pyrex injector equipped with a fritted end. The gas phase NO_2 reactant was monitored directly (i.e., the reactant gas was introduced directly into the differentially pumped chamber without any pre-treatment or pre-concentration) using a quadrupole mass spectrometer. The molecular mass signal of the NO_2 reactant gas (m/z= 46) was monitored.

The uptake coefficients for NO_2 were determined by measuring the quantity of the NO_2 reactant gas absorbed by the organic film [43,42]. The trace gas loss in the flow tube can be measured as a function of the position (distance) of the movable inlet tube (injector) i.e., as a function of the gas / solid exposure time t. The maximum length l of the interaction zone (maximum length that the injector could be retracted) was about 30 cm. As shown in equation (I) below, the measured loss rate can be interpreted in terms of a first order process with respect to the gas phase concentration of the reactant.

$$\frac{n - \Delta n}{n} = \exp\left[- k_w t\right] \qquad (I)$$

In equation (I) t is the average carrier gas residence time and k_w is the first order rate coefficient for the reaction at the film surface. The first order rate coefficient k_w is related to the uptake coefficient by

$$k_w = \frac{\gamma < c >}{2 r_{tube}} \qquad (II)$$

In equation (II), r_{tube}, γ, and $<c>$ are the flow tube radius, uptake coefficient and average molecular velocity, respectively.

Initial concentrations of each component in the reaction mixture were determined from measurements of the appropriate mass flow rates, vapour pressure, and the total pressure. The mass flow rates were determined using Brooks electronic mass flow meters which had ranges of 20 to 1000 standard cm^3 min^{-1} (SCCM). The NO_2/He standard mix and the He buffer gas were allowed to flow directly from their high pressure storage tanks.

Water vapour was added by bubbling the helium gas through a flask containing deionized H_2O.
Two mercury HPK lamps (Cathodeon), with an arc length of about 5 cm were mounted parallel above and below the horizontal reactor. The two lamps were about 3 cm, away from the thermostated pyrex flowtube. These lamps and the flowtube were surrounded by an aluminium jacket in order to increase the homogeneity of the light inside the reactor.
The solid organic film was prepared using two complementary methods. In the first method, the organic solid was heated in an air tight flask while a small flow of nitrogen gas was allowed to pass through. Then, the organic vapour carried by the nitrogen carrier was "injected" using Teflon tubing and deposited directly on the colder insert (see Figure 1) inner surface. In the second method, a known quantity of the organic was dissolved in methanol. Then, a 5 ml aliquot of the organic+methanol solution was placed inside the rotating insert. The insert was then dried by allowing a small flow of nitrogen to pass through the tube.

b) Flow tube experiments with LOPAP and Chemiluminiscence NO_x Detector

Further investigations were performed at lower, atmospherically more relevant NO_2 concentrations in synthetic air by using the sensitive direct analysis of the produced HONO by a HONO-analyzer (Long Path Absorption Photometer: LOPAP; described below) or alternatively by a indirect detection of the produced HONO by means of a NO/NO_x-chemiluminescence detector (CLD, Ecophysics, model CLD77AM coupled to a molybdenum converter at 400°C reducing HONO and NO_2 to NO), in combination with a sodium carbonate denuder tube for removing HONO from the gas stream. This molybdenum converter/chemiluminescence detection system principally measures the NO_y-species NO, NO_2, and HONO with an equal analytical response. The sodium carbonate denuder tube (50 cm × 0.8 cm ID glass tube) may either be switched into the sampling line to measure the sum of the species NO, NO_2 or may be bypassed that the CLD signal accounts for the sum of the species NO, NO_2 and HONO. The HONO concentration can therefore be expressed as the difference of the CLD-signal without and with carbonate denuder in the sampling line[24]. The NO concentration can be obtained from the detector signal, when the molybdenum converter is bypassed.
The photoreactor employed was a 50 cm × 0.8 cm ID Duran glass tube installed in an air cooled lamp housing holding 7 fluorescence lamps in a circular arrangement surrounding the reactor tube. The lamps used are Phillips Cleo Compact tanning lamps (48 cm × 2 cm), which emit light as a continuous band in the 300-420 nm (λmax = 354 nm) spectral region (90 % of the light power) and in the discrete Hg-lines at 436 nm, 546 nm, and 578 nm (9.8 % of the light power). The spectral irradiance E(λ) reaching the reactor surface was measured with a LI-COR 1800 hemisperical, cosine corrected spectroradiometer. The total irradiance (250-800 nm) is 150 Watt m^{-2} at the reactor surface. The inner surface of the tubular flow reactor was coated with a film of organic compounds. This surface was sandblasted to prevent droplet formation during the coating procedure and therefore reach a relatively homogeneous distribution of the organic test compound on the reactor walls. The organic coatings on the reactor wall were produced by gently drying 0.5 ml aliquots of solutions of the organic compounds (either aqueous solutions or solutions in ethanol or dichloromethane; depending on the solubility of the solute) dispersed on the reactor walls in a nitrogen stream at room temperature.
The carrier gas flow (synthetic air) and the NO_2 addition, from a 959 ppb mixture in synthetic air (Carbagas AG, Switzerland), were controlled by mass flow controllers. Usually total flows rates of about 2.5 liters per minute at ambient pressure were used leading to gas residence times of about 0.5 seconds in the photoreactor. The reactor temperature was 30-32 ºC during irradiation. The NO_2 concentrations were adjusted normally around 20 ppb, a typical average concentration found in the atmosphere in densely populated areas within Europe. All experiments were performed at about 20 % relative humidity. In order to prevent HONO eventually present in the NO_2-supply from entering the coated wall flow tube, an additional carbonate denuder was placed upstream of the flow reactor.

LOPAP instrument
For the measurement of nitrous acid (HONO) a new, very sensitive instrument (LOPAP: Long Path Absorption Photometer) was used, which is described in detail elsewhere [44,45]. Briefly, HONO is sampled in a stripping coil by a fast chemical reaction and converted into an azo dye which is photometrically detected in long path absorption inside a special Teflon tubing. During the measurements the instrument had an integrated time resolution of ~2.5 min and a detection limit of 5 pptV. Caused by the two-channel concept of the instrument all tested interferences including the combined one against NO_2 and unknown semi-volatile diesel exhaust components [22] can be neglected [45]. In a recent intercomparison campaign with a DOAS instrument in which the same air masses were analysed for the first time, an excellent agreement was obtained [46] also during the day.

Reagents

Following organic test reagents were obtained from the commercial suppliers with the purity given below and used without further purification: 4-benzoylbenzoic acid (4-BBA, Fluka; ≥ 98%), perylene (PER, Fluka; ≥ 99%), 4-hydroxy-3,5-dimethoxy benzoic acid (syringic acid, SYR, Fluka; ≥ 97%), 3,7-dihydroxy-2-naphtoic acid (3,7-DHNA, Fluka; ≥ 95%), potassium iodide (Fluka; ≥ 99%), 3,4-dihydroxy-phenylacetic acid (3,4-DHPA, Fluka ; ≥ 98%), Catechol (Aldrich, 99%), anthracene (Aldrich, 99%), benzophenone (Aldrich, 99%), anthrarobin (Aldrich, 85%). The solvents used are analytical grade, and water was purified with a Millipore Milli-Q water system to a resistivity ≤0.054 μS cm^{-1}.

Results and Discussion

Uptake of NO_2 under dry and dark conditions

The uptake on bare glass was beyond the sensitivity of our horizontal coated wall reactor with MS detection, which means that the uptake coefficient was below the detection limit of a few times 10^{-7}. Only a physical adsorption was observed i.e., the surface exposed by the glass flow tube was rapidly covered and saturated by NO_2 molecules. At this stage, no more uptake occurred on this surface. As the surface could be exposed stepwise to gas phase NO_2, we could measure adsorption and desorption isotherms. By this we could observe a fully reversible uptake on the glass surfaces i.e., in the dark and at low relative humidity i.e., rh below 1%), there was no reaction on the bare glass surface.
The uptake of NO_2 in the dark was also studied on various pure organic surfaces i.e., on catechol, anthracene, benzophenone, anthrarobin.
As an example, the raw data during a NO_2 uptake experiment on a pure catechol surface is shown in Figure 2. When the organic surface was exposed to gaseous NO_2, we first observed a rapid decrease of the MS signal at m/z 46 (i.e., corresponding to the NO_2 molecular mass) which recovered to its original level within a few minutes. This timescale was of course depending on the actual flow rate used in the experiment and the NO_2 concentration. However, as the recovery of the MS signal was rapid, low flow rates, of about 150 mL min^{-1}, were typically used. Even under these conditions, the gas phase concentration

of NO_2 first decreased and recovered very rapidly to its original level after exposure to an organic surface.

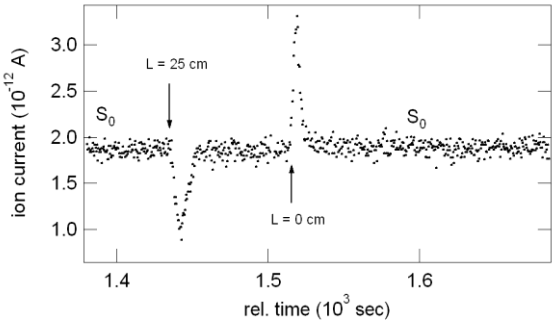

Figure 2. Typical NO_2 signal (m/z= 46) observed for the uptake of NO_2 gas on solid catechol under "dark" conditions. Experimental conditions are 0% RH; p=760 Torr; T=298 K; $[NO_2]_0$=4.9 x 10^{14} molecules cm^3. A decrease in the NO_2 signal is observed when the injector is moved back to L=25 cm. The signal is observed to recover to its original S_0 level within seconds. Once the inlet is moved all the way in (L=0 cm) so that the catechol surface is not exposed to the absorbent gas, the signal is observed to increase to greater than S_0 since the absorbed NO_2 gas desorbs from the catechol surface into the carrier gas and adds to the carrier gas.

This means that the organic surfaces were very rapidly saturated with NO_2 molecules, as this was the case with the bare glass surface. In our setup the NO_2 injector can be pulled back at its original position in which the organic surface is only flushed with the carrier gas (i.e., helium in these experiments). When this was done, we observed a rapid increase of the MS signal at m/z 46, which then decayed back to its original level. This corresponds to the desorption of physically adsorbed NO_2 molecules. By integrating the area below these peaks, we can determine the number of molecules being adsorbed or being desorbed. We observed that theses quantities are, within experimental uncertainty, equal which means again that under dry conditions, NO_2 only physically adsorbs on these pure organic surfaces (as on the bare glass tube but in slightly smaller amounts).

As NO_2 only physically adsorbs on these catechol surfaces, we were unable to determine any reliable uptake coefficients, which were below or too close to our detection limit of a few times 10^{-7}.

Similar observations have been made on a surface made of anthrarobin (1,2,10-trihydroxyanthracene) i.e., NO_2 only physically adsorbs on these surfaces with uptake coefficients, which were below or too close to our detection limit of a few times 10^{-7}.

On anthracene surfaces, we observed a similar behaviour but we observed also a small dark reaction. In this case, when NO_2 was exposed to the organic surface, its gas phase concentration rapidly decayed and then started to recover to its original level. However, with anthracene, NO_2 never reached again its initial concentration, within our experimental conditions, but reached a plateau which is an evidence that at long enough gas/solid contact times, the uptake is driven by a slow dark reaction. However, this was observed to slow down at long reaction times i.e., the plateau is not totally time independent, which means that there is a deactivation of the surface during the course of the experiment. Similar observations were made in the case of benzophenone, for which an uptake coefficient of 0.3×10^{-6} was determined. All results are summarised in Table I.

Humidity and dark chemistry

While all experiments described above were performed under dry conditions (i.e., rh < 1%), we observed that adding water vapour into the gas flow lead to an increased uptake of NO_2 by at least a factor of 3 when the humidity was increased to more than 40 %. And this was observed for all materials studied. It appears certainly that water adsorbs on our films changing the properties of the surfaces and its ability to react with NO_2. Visual inspection showed that some of the films deliquesced at high humidity. It seems clear that the total amount of water taken up into the film has an influence on its reactivity, as the presence of an aqueous phase could enhance the liquid phase mechanisms with NO_2 [27,24]. However, also in this case a time dependent uptake was observed i.e., the surface was deactivated slowly with increasing reaction time, similar to the observations made by Arens et al. [27] on solid anthrarobin.

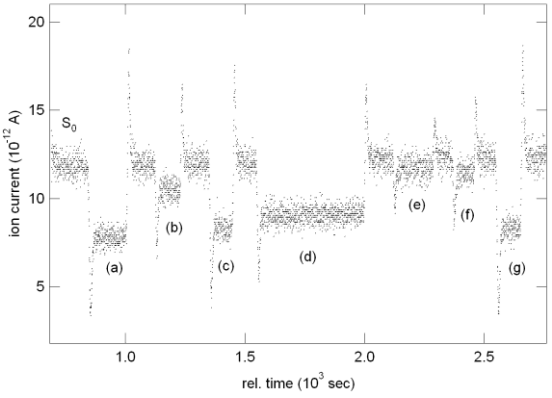

Figure 3. Typical NO_2 signal (m/z= 46) observed for the uptake of NO_2 gas on solid catechol in the presence of light. Experimental conditions are 0% RH, p=760 Torr and T=298 K. $[NO_2]_0$= 1 x 10^{15} molec. cm^3 ; injector length L (in cm) is (a) 32.5; (b) 13.8; (c) 26.0; (d) 19.8; (e) 6.5; (f) 10.5; (g) 33.8. γ = 2.1 x 10^{-6}

Surface photochemistry

Figure 3 shows the raw data for an uptake experiment on a catechol surface when the pyrex flowtube was irradiated by the output of the mercury lamps . This has to be compared with data shown in Figure 2 (corresponding experiment but in the dark). It is obvious that in the dark only physical adsorption is occuring while under irradiation the uptake of NO_2 is driven by a chemical reaction on the solid film. In fact, in this later case the uptake coefficient is no more time dependent, as the NO_2 concentration, when exposed to the irradiated flowtube, decreases rapidly and reaches a plateau after a few seconds. Here the quantity of NO_2 that has reacted is depending "only" on the surface exposed to the gas phase. The uptake coefficient measured in this case is about 10^{-6} i.e., at least an order of magnitude larger than without light.

The light induced effects for the other organics is less pronounced but mainly visible through the removal of any time dependence in the uptake coefficient. The main effect of light was therefore to eliminate any sign of deactivation of the surfaces within the experimental time scales.

Not only the magnitude and time dependence of the uptake of NO_2 was increased under irradiation, we also observed MS-signals from a potential gas phase product. The observation is that both MS-signal traces for m/z= 30 (NO^+-ion) and m/z= 46 (NO_2^+-ion) are well correlated in the presence of unreacted NO_2 at varying concentrations. However, when NO_2 was reacted with irradiated organic films the signal at m/z= 30 rised, whereas the sinal at m/z= 46 decayed. This was interpreted as a product signal was interfering with the signal of mass 30, whereas mass 46 was not influenced. Potential reaction products showing mass signals at m/z=30 are NO (from a surface photolysis of NO_2) or HONO (from reduction of NO_2).

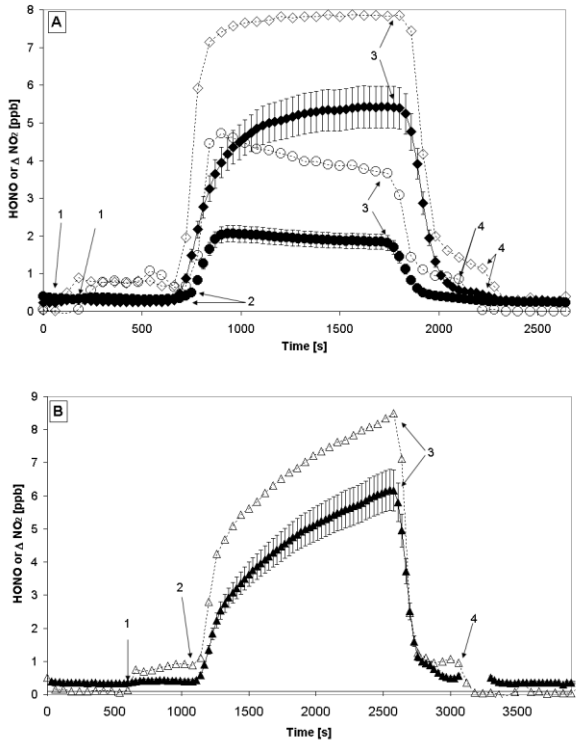

Fig. 5 Concentration of the reaction product HONO and change of the NO_2 concentration during irradiation (300-420 nm) of organic films. Results from three different experiments are shown. **Panel A:** An experiment where a film of 4-benzoyl-benzoate sodium salt (1 mg on 125 cm^2 sandblasted Duran glass) is irradiated (filled circles: HONO concentration; empty circles: loss of NO_2, i.e. $NO_2(t=0)$-$NO_2(t)$) and an experiment where a mixed film of 4-benzoyl-benzoate sodium salt (1 mg on 125 cm^2 glass surface) and syringic acid (0.5 mg on 125 cm^2 glass surface) is irradiated (filled diamonds: HONO concentration; empty diamonds: loss of NO_2, i.e. $NO_2(t=0)$-$NO_2(t)$). **Panel B:** An irradiation of 3,7-dihydroxy-2-naphtoic acid (1 mg on 125 cm^2 glass surface; filled triangles: HONO concentration; empty triangles: loss of NO_2, i.e. $NO_2(t=0)$-$NO_2(t)$).
The numbers given in the figures represent following steps in the course of the experiments: (1) The coated reactor was switched into the NO_2 stream ($NO_2(t=0)$= 19 ppb); (2) the light source (300-420 nm) was switched on; (3) the light source was switched off; and (4) the coated reactor was removed from the NO_2 stream.

To determine if the product formed was HONO or NO, we inserted a sodium carbonate coated trap in the gas line between the flow tube and the MS that would remove any traces of HONO from the gas phase. With the trap in-line, the mass 30 follows mass 46 which can be taken as an indirect evidence that HONO is photochemically formed during the interactions of NO_2 and the various organics films. Note however, that the production of HONO was only observed when the gas was humidified.
It is however very difficult from these experiments to draw any conclusions about the reaction mechanism simply because we are unable to distinguish between photochemistry of adsorbed NO_y species and photochemistry involving the organic compounds. Aditionally these experiments were performed at higher NO_2 concentrations than typically found in atmospheric environments.
While the experiments with mass spectrometric detection revealed that HONO might be a product of a photoenhanced reaction of NO_2 with the organic species investigated, further experiments were performed with specific and sensitive HONO detection, at low concentrations of NO_2. Three different types of light absorbing organic species have been investigated. These are

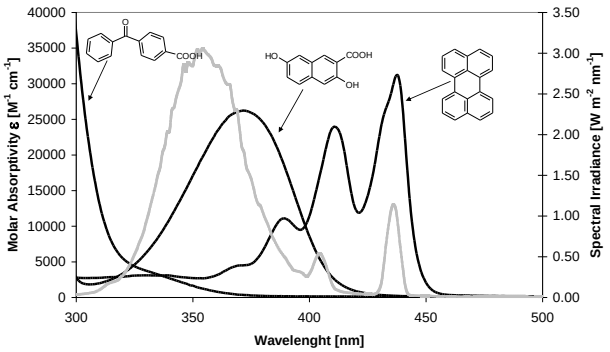

Fig. 4 Absorption spectra (molar absorptivities ε) of the investigated organic light absorbers 4-benzoylbenzoic acid (4-BBA), 3,7-dihydroxy-2-naphtoic acid (3,7-DHNA) and perylene (PER), overlaid with with the spectral irradiance of the light source (Philips Cleo Compact fluorescence lamps, grey line). 4-BBA and 3,7-DHNA are recorded in phosphate buffered aqueous solution (pH=7), PER is recorded in dichlormethane.

4-benzoylbenzoic acid (4-BBA) and its sodium salt, 3,7-dihydroxy-2-naphtoic acid (3,7-DHNA) and perylene (PER). 4-BBA is an analogue of benzophenone, bearing an extra organic acid substituent. This compound has been used instead of benzophenone, as it is less volatile and therefore the produced films are more stable during the experiments. 4-BBA was selected as it is known to form excited triplet states in high yields when irradiated in the UV-A spectral region in benzene and in water containing solutions [47,48]. Contrary PER was selected as a mechanistical probe molecule, as it has a high fluorescence quantum yield in benzene solutions or alcohol solutions and hardly forms excited triplet states [49,50,48]. However, in our experiments these absorbers are investigated as pure organic films, which were exposed to humid air (relative humidity of about 20%), therefore the triplet and fluorescence yields of the absorbers may be significantly altered from those reported in the literature for benzene or aqueous solutions. As a third UV-A absorbing species 3,7-DHNA was chosen, as hydroxylated aromatic compounds are known to react with NO_2 in aqueous solution or on wetted surfaces to form nitrite ions and aryloxy radicals in a dark reaction [23,27,24,34]. Our aim was to test if this reaction could be enhanced in presence of light. In Figure 4 the absorption spectra of the three compounds are shown in comparison with the spectral irradiance measured at the reactor surface.
Two additional model compounds m 3,4-dihydroxyphenylacetic acid (3,4-DHPAA) and 4-hydroxy-3,5-dimethoxybenzoic acid (syringic acid, SYR) were selected as electron donors. Both compounds are electron donor substituted phenols, which are on one hand capable to reduce NO_2 in aqueous solutions [34] and which on the other hand can reduce photochemically excited triplet states of aromatic ketones, such as 4-BBA [51-53]. Both compounds hardly absorb light in the spectral region above 300 nm. For comparison an inorganic electron donor, potassium iodide, was examined additionally.
In Table II the observation of the change of the NO_2 concentration and the formation of HONO have been summarized for the experiments with different organic films. All experiments have been performed at a relative humidity of about 20 % in synthetic air at atmospheric pressure.
Figure 5 shows the concentration evolution of NO_2 and HONO during a typical experiment, where NO_2 was measured with the chemiluminescence detector and HONO was measured with the long path absorption photometer (LOPAP).
It is obvious from Table II and Figure 5, that a significant depletion of NO_2 occurred on the organic substrate surfaces

during irradiation. The direct measurement of gaseous HONO with the LOPAP-analyser clearly shows that a large fraction of NO_2 taken up was converted into HONO, in line with the experiments shown above and with an earlier study on dark reactions of NO_2 on anthrarobin (Arens et al., 2002). A small production of HONO was also observed during dark exposure of the organic films towards NO_2, but the HONO-yield increased by more than an order of magnitude during irradiation. It appears that the photochemical production of HONO is strongly dependent on the type of organic species examined. For perylene no photochemical production of HONO was observed, whereas 4-BBA and 3,7-DHNA are efficiently reacting with NO_2 and produced significant amounts of HONO during irradiation. From Figure 5 it can be seen that for 4-BBA the yield of HONO only accounts for roughly 50 % of the reacted NO_2. For 3,7-DHNA the observed gaseous HONO accounts for about 75 % of the reacted NO_2. As shown in Table II and discussed below for some mixed organic coatings containing 4-BBA nearly 100 % of the reacted NO_2 is converted into HONO.

Another difference between 4-BBA and 3,7-DHNA is that 4-BBA shows the highest reactivity at the beginning of the irradiation, whereas the reactivity of 3,7-DHNA increases during the course of an irradiation. Therefore it appears that 3,7-DHNA is converted into more reactive product species during the course of its photochemical degradation. As stable reaction products of 3,7-DHNA higher oxidised products as hydroxynapthoquinones, nitroaromatic compounds or oxydised monoaromatic compounds might be expected [54-57], which are stronger absorbers or have different photochemical properties.

The model electron donors used in this study, SYR, 3,4-DHPAA, and potassium iodide, are able to react directly with NO_2 in a dark reaction yielding nitrite or nitrous acid. This can be seen clearly for the experiment with potassium iodide coating, where a considerable dark reaction occurred. However, the reaction was not significantly photoenhanced under our irradiation conditions. For the phenolic compounds, SYR and 3,4-DHPAA a slight HONO-production occurred upon irradiation. As these compounds are hardly absorbing under the given light conditions, this is somewhat surprising and might be related to impurities present in these compounds or on the reactor wall or to absorbing species formed during the exposure of the compounds to the NO_2/synthetic air mixture in the reactor.

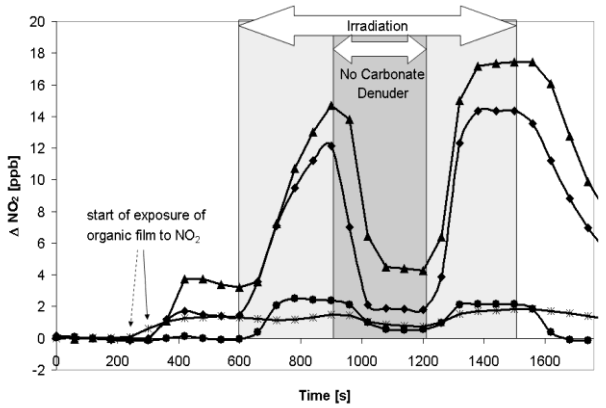

Figure 6: Change of the NO_2 concentration during irradiation (300-420 nm) of different organic films. The displayed unit Δ NO_x is the loss of NO_x in the coated wall reactor and in the carbonate denuder (i.e. $NO_x(t=0)$-$NO_x(t)$). The figure illustrates the steps of a typical experiments using the carbonate denuder technique for the CLD-detection of NO_2 and HONO. At time 300 s the coated wall reactor was switched into a stream of NO_2 in synthetic air (20 ± ppb). At time 600 s the reactor is illuminated until time 1500 s. At times 900 s to 1200 s the carbonate denuder preventing HONO from entering the CLD detector is bypassed. The concentration steps starting at the times 900 s and 1200 s are a indirect measure of the HONO concentration in the reactor effluent. Results from four different experiments are shown: (M) Exposure of a film of 4-benzoylbenzoic acid (1 mg per 125 cm^2 surface); (*) Exposure of a film of 3,4-dihydroxyphenylacetic acid (1 mg per 125 cm^2 surface); (▲) Exposure of a internally mixed film of 4-benzoylbenzoic and 3,4-dyhydroxyphenylacetic acid (1 mg and 0.5 mg per 125 cm^2 surface, respectively; (♦) Exposure of a internally mixed film of 4-benzoylbenzoic and 3,4-dyhydroxyphenylacetic acid (1 mg of both compounds per 125 cm^2 surface).

Proposed reaction mechanism

Using the combination of a Pyrex flow tube and a mercury lamp, we are initiating photochemistry at wavelengths longer than 300 nm. Indeed, the triple Pyrex walled flow tube would have filtered out any wavelength shorter than 300 nm. In addition, the output of the lamp will be mainly around 366 nm. For the experiments illuminated with the Philips Cleo Compact Fluorescence lamps the spectral irradiance at the reactor surface has been measured (see Figure 4). Under the assumption of an isotropic radiation in the reactor (e.g. the flow tube is surrounded by 7 fluorescence lamps in a cyclic arrangement mounted in a reflecting aluminium box) the actinic flux in the reactor is estimated after the procedure of Madronich [58] as four times the measured 2π-spectral irradiance, neglecting any influence of the glass reactor walls. Using the actinic flux derived this way and using the IUPAC recommendations for the cross-sections and quantum yields [59], we would calculate the photolysis frequencies $J(NO_2)$ as 0.046 s^{-1}, J(HONO) as 0.011 s^{-1} and $J(HNO_3)$ as 1.8×10^{-6} s^{-1} for the respective gaseous species. For the aqueous nitrate ion, a somewhat higher photolysis frequency of $J(NO_3^-{}_{aq})$= 2.5 $\times10^{-6}$ s^{-1} is expected based on the literature absorption spectra and quantum yields [60]. We also determined $J(NO_2)$ experimentally by the photolysis of NO_2 in air and the measurement of the reaction product NO as 0.024 ± 0.007 s^{-1}. Therefore, our model overestimates the actual actinic fluxes in the reactor by roughly a factor of 2, which might have resulted mainly from neglecting of absorbance and the light reflection of the Duran glass flow tube and the simplified representation of the radiation conditions in the reactor. Nevertheless, the calculated photolysis frequencies indicate that direct HNO_3/NO_3^- photolysis should be insignificant even when we would assume that 10 % of the initial NO_2 concentration would hypothetically react to HNO_3 in the dark and accumulate on the reactor wall and would then photo-dissociate with a hypothetical unity quantum yield to form HONO, as suggested by Ramazan et al. [39]. In our experiments this explanation is likely not valid, as the reservoir of adsorbed HNO_3 would be to limited to explain the HONO-formation, because an experiment to experiment carry-over of adsorbed HNO_3, as commonly observed in smog chamber experiments [39] , is unlikely in our experiments, due to the multi-step soaking and rinsing procedure used to clean our reactors. In addition, it was clearly demonstrated that no nitrate is formed in the electron transfer reactions between hydroxylated aromatic compounds and NO_2 in the dark [27]. This excludes nitrate formation on the organic substrates before irradiation.

The photolysis of gaseous NO_2 and HONO seems to be unimportant under the given flow tube conditions (0.5 s residence time). This is in agreement with our finding that NO is not produced in significant amounts in our experiments.

No significant photoenhancement of the reaction of NO_2 with the clean glass surface was observed under humid conditions, in good agreement with previous studies, which showed that reaction (2) is not photoenhanced [39,40]. Due to the fact that the mechanism operated down to very low concentrations of NO_2, the involvement of N_2O_4 (and subsequent photochemistry) is unlikely.

The stoichiometry of the formation of HONO from NO_2 in the 4-BBA photosensitized reaction (see Table II) with a HONO yield up to 100 % shows that the reaction cannot be explained as a catalysed disproportionation of NO_2 on wet surfaces (equation 2,

see introduction) as soon as suitable electron donors are present in the system, Therefore, the primary electron donor must be a constituent of the organic films.

From the data presented in Table I and II and Figures 5 and 6 it appears that NO_2 is transformed in an efficient and coating specific photoreaction on organically coated glass surfaces. Very reactive coatings were obtained from 4-BBA, especially when it was mixed with an electron donor, such as a phenolic compound. In the given experiments the light is primarily absorbed by 4-BBA and therefore we suggest a mechanism, where this benzophenone derivate acts as a photosensitizer for the reduction of NO_2. The proposed reaction mechanism is depicted in Figure 7. It is based on the findings from photochemical experiments in solution [51,52,48], which conclude that the photoexcitation of benzophenones produces excited triplet states of benzophenone in near unity yield. These triplet states act as one electron oxidants and react with electron donor substituted phenols in near diffusion controlled rates [61,53,62]. The resulting products are phenoxy radicals and reduced benzophenones (diphenyl ketyl radicals). Therefore this photosensitized reaction generates reactive radical intermediates which are though to be reactive towards NO_2. The ketyl radical of benzophenone is a short lived reductant, which is generally assumed to react with dissolved oxygen in aerated aqueous solution experiments [63,62] to form O_2^-/HO_2 radicals. Such reaction systems have been investigated by Anastasio et al. [64], who irradiated mixtures of aromatic ketones and aldehydes in dilute aqueous solution. They observed a distinct formation of H_2O_2, when phenolic compounds were added to the solution of the aromatic ketone photosensitizers, and proposed that H_2O_2 is formed from the disproportionation of O_2^-/HO_2 radicals resulting from the reaction of the intermediate ketyl radicals with oxygen (equations 3 and 4).

$$PhOH + O_2 \xrightarrow{\text{sensitizer } +h\nu} PhO\bullet + HO_2 \qquad (3)$$

$$2HO_2 / O_2^- \rightarrow H_2O_2 + O_2 \qquad (4)$$

The aromatic photosensitizer molecules were only slowly consumed in the reactions and acted therefore as photocatalysts mediating the reduction of oxygen by phenols. However the yields of H_2O_2 were lower by a factor of 2.5 than expected from the given mechanism and the oxidation rate of the phenols. This indicates that dissolved O_2 might not be viewed as the sole possible final electron acceptor in such reaction systems. As indicated in Figure 7 beneath oxygen also organic constituents and in our case NO_2 could act as final electron acceptors. It also seems possible, that NO_2 can be reduced by the intermediate HO_2/O_2^-radical produced from reaction (3), as both reactions (5) and (6) [65]

$$O_2^- + NO_2 \rightarrow O_2NOO^- \qquad (5)$$

$$k(5) = 4.5\times10^9\ M^{-1}\ s^{-1}$$

$$HO_2 + NO_2 \rightarrow O_2NOOH \qquad (6)$$

$$k(6) = 1.8\times10^9\ M^{-1}\ s^{-1}$$

are significantly faster than the disproportionation reactions of HO_2/O_2^- over the whole pH range, but it is not clear how fast the reaction products the peroxynitric acid/peroxynitrate decay into HONO/NO_2^- and O_2 under our reaction conditions, as in aqueous solution only the deprotonated form (pK_a= 5.85) decayed rapidly (lifetime τ= 1 s)[Logager and Sehested, 1993]. Therefore, we propose that NO_2 is reduced in the present system by reductants produced during the photosensitized oxidation of phenols. These reductants might be the ketyl radical formed from 4-BBA, the superoxide/hydroperoxyl radical formed from the reaction of the

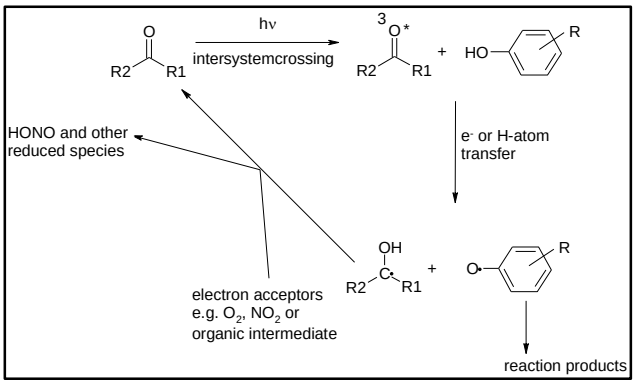

Figure 7: Proposed reaction mechanism for the photoreduction of NO_2 to HONO in the presence of 4-BBA (absorbing photosensitizer) and a substituted phenol (electron donor)

ketyl radical with oxygen or reduced intermediates stemming from subsequent reactions of the ketyl radicals with organic constituents (phenol degradation intermediates) present in the organic films.

The experiments employing iodide as the electron donor were conducted to investigate an alternative route to produce the ketyl radical of 4-BBA. [66,67]. Iodide reacts with excited triplets of 4-BBA in a near diffusion controlled rate to form a charge-transfer exciplex which can react (in presence of high concentrations of iodide) with an additional iodide ion and subsequently dissociate into the ketyl radical and a diiodide ion (equation 7 and 8).

$$4-BBA + I^- \xrightarrow{h\nu} {}^3[4-BBA^-I] \qquad (7)$$

$${}^3[4-BBA^-I] + I^- \rightarrow 4-BBA^- + I_2^- \qquad (8)$$

The results from these experiments (Table II) show that the phototransformation of NO_2→ HONO is also effective, when the electron donors is not a phenolic compound. This indicates that neither radical oxidation intermediates of the phenols nor products of the phenolic oxidation (for example quinones) are necessary for the photoreduction of NO_2→HONO. This is a strong indication that the diphenylketyl radical (protonated and/or deprotonated form) is a key species in the reduction of NO_2. Furthermore, the experiment with iodide showed that energy transfer reaction between triplet 4-BBA and the probe phenols in the ground state (equation 9) is not essential in the reaction system. This type of energy transfer reaction might occur if the lowest triplet state energy of the phenols is lower than that of 4-BBA (68.3 kcal/mol [66]). Measurements by Canonica et al. [53] for some selected substituted phenols showed that they had higher triplet energies than 4-BBA.

$${}^3 4-BBA + PhOH \rightarrow 4-BBA + {}^3PhOH \qquad (9)$$

In order to obtain a more quantitative understanding of the ongoing reactions the overall quantum yields of the HONO-formation are estimated by using the solution UV/VIS-absorption spectra and the spectral irradiance measured at the outer surface of the reactor as presented in Figure 4. The estimated total photon absorptions of 0.5 mg PER-, 1 mg 4-BBA- and 1 mg 3,7-DHNA-films are 1.6×10^{-6}, 1.0×10^{-6} and 4.6×10^{-6} Einstein per second, respectively. Therefore, the highest overall quantum yields reached in the present study (for the mixtures of 4-BBA and 3,4-DHPAA and 20 ppb of NO_2) are estimated to be around 4.1×10^{-5}. This overall quantum yield is of course depending on the exact parameters in our experiments, as

for example the NO_2 concentrations, the thickness and homogeneity of the organic films, but should give an impression about the effectiveness of the observed photoreactions. Clearly, the low quantum yields for the HONO-production leave room for a multitude of photophysical processes and photochemical reactions of the excited 4-BBA molecules and the conversion of $NO_2 \rightarrow$HONO is not more than a side reaction. The proposed mechanism is therefore rather uncertain, but it explains a number of the observed characteristics of the reaction, i.e. (i) the higher reactivity of the 4-BBA-mixtures than of the perylene mixtures, (ii) the acceleration of the photoreaction of 4-BBA with NO_2 in presence of non-absorbing electron donors, (iii) the low photo enhancement of the reaction of NO_2 with the electron donors in absence of 4-BBA and (iv) the high conversion yields of $NO_2 \rightarrow$HONO indicating that the reducing agent is photoproduced in the organic film.

Atmospheric implications

Based on experimental evidence presented in this study, photoinduced conversion of NO_2 into HONO has been observed on organic films, which exceeds the rate of the dark reaction by one order of magnitude (see Fig. 5) and that of reaction (2) by even more than one order of magnitude under our experimental conditions. Uptake coefficients observed here easily reach the 10^{-6} range or higher, with HONO yields between 50 and close to 100% with an artificial irradiance comparable to the irradiance in the wavelength interval of 300-400 nm at the Earth surface under 0° Zenith angle. From field measurements, it was recently estimated that there is an unknown daytime source of HONO which exceeds the night time source by a factor of 20 [37]. Since the night time formation could be very well explained by emission and heterogeneous HONO formation on ground surfaces by reaction (2) [9], a photoinduced enhancement of the rate of HONO formation by at least one order of magnitude observed in this study, would help to explain the missing daytime source. The species under study here are representatives of decomposition products of major structural components of vegetation and are ubiquitously distributed in the environment. In addition, the absorbing species necessary to provide excited molecules for initiating the primary electron transfer process from the phenolic species may be found among the oxidation products of the same species family, i.e., the natural oxidation chain produces the necessary ingredients of the suggested mechanism continuously. Note that such species are also present in the atmospheric aerosol, from the photochemical degradation of aromatics or as components of biomass burning aerosol.
Grannas et al. [68] report significant contributions of vanillyl phenols, syringyl phenols, cinnamyl phenols, p-hydroxyacetophenone, p-hydroxybenzaldehyde (lignin derived metabolites) to the organic carbon content in the arctic snow-pack. It seems therefore likely that the mechanism suggested here is also operating under those conditions. It could then even explain the high HONO yields observed in Arctic regions, since these high yields are in contradiction to the known photochemisty of nitrate. In the laboratory, the effective yield for nitrite formation was found to be two orders of magnitude smaller compared to the NO_2 formation [69], whereas in arctic regions $HONO/NO_2$ ratios up to 1:2 are observed [70]. So probably, the NO_2 formed in the nitrate photolysis is efficiently converted into HONO even on polar snow surfaces by the mechanism suggested here.

Acknowledgement

The support by the French program PRIMEQUAL2 for the project SHONO and by the Swiss National Science Foundation are gratefully acknowledged

[(#)] *Now at Université de Provence, TRACES, Centre de Saint Jérôme, Case 512, 13397 Marseille cedex 20, Tel. : (+33)(0)4 91 28 86 43. E-mail : Rafal.Strekowski@up.univ-mrs.fr*

References

1 D. Perner; Platt, U. *Geophys. Res. Lett.*, 1979, **6**, 917.
2 G. W. Harris; Carter, W. P. L.; Winer, A. M.; Pitts, J. N., Jr.; Platt, U.; Perner, D. *Environ. Sci. Technol.*, 1982, **16**, 414.
3 R. M. Harrison; Peak, J. D.; Collins, G. M. *J. Geophys. Res.*, 1996, **101**, 14429.
4 B. Alicke; Platt, U.; Stutz, J. *J. Geophys. Res.*, 2002, **107**, LOP9/1.
5 X. Zhou; Civerolo, K.; Dai, H.; Huang, G.; Schwab, J.; Demerjian, K. *J. Geophys. Res.*, 2002, **107**, ACH13/1.
6 B. Alicke; Geyer, A.; Hofzumahaus, A.; Holland, F.; Konrad, S.; Paetz, H. W.; Schaefer, J.; Stutz, J.; Volz-Thomas, A.; Platt, U. *J. Geophys. Res.*, 2003, **108**, PHO 3/1.
7 B. Aumont; Chervier, F.; Laval, S. *Atmos. Environ.*, 2003, **37**, 487.
8 X. Ren; Harder, H.; Martinez, M.; Lesher, R. L.; Oliger, A.; Simpas, J. B.; Brune, W. H.; Schwab, J. J.; Demerjian, K. L.; He, Y.; Zhou, X.; Gao, H. *Atmos. Environ.*, 2003, **37**, 3639.
9 B. Vogel; Vogel, H.; Kleffmann, J.; Kurtenbach, R. *Atmos. Environ.*, 2003, **37**, 2957.
10 J. G. Calvert; Yarwood, G.; Dunker, A. M. *Res. Chem. Intermed.*, 1994, **20**, 463.
11 R. Kurtenbach; Becker, K. H.; Gomes, J. A. G.; Kleffmann, J.; Lörzer, J. C.; Spittler, M.; Wiesen, P.; Ackermann, R.; Geyer, A.; Platt, U. *Atmos. Environ.*, 2001, **35**, 3385.
12 M. Ammann; Kalberer, M.; Jost, D. T.; Tobler, L.; Rossler, E.; Piguet, D.; Gäggeler, H. W.; Baltensperger, U. *Nature*, 1998, **395**, 157.
13 A. Gerecke; Thielmann, A.; Gutzwiller, L.; Rossi, M. J. *Geophys. Res. Lett.*, 1998, **25**, 2453.
14 J. Kleffmann; Becker, K. H.; Lackhoff, M.; Wiesen, P. *Phys. Chem. Chem. Phys.*, 1999, **1**, 5443.
15 F. Arens; Gutzwiller, L.; Baltensperger, U.; Gäggeler, H. W.; Ammann, M. *Environ. Sci. Technol.*, 2001, **35**, 2191.
16 R. M. Harrison; Kitto, A.-M. N. *Atmos. Environ.*, 1994, **28**, 1089.
17 J. Kleffmann; Becker, K. H.; Wiesen, P. *Atmos. Environ.*, 1998, **32**, 2721.
18 N. A. Saliba; Mochida, M.; Finlayson-Pitts, B. J. *Geophys. Res. Lett.*, 2000, **27**, 3229.
19 J. Kleffmann; Benter, T.; Wiesen, P. *J. Phys. Chem. A*, 2004, **108**, 5793.
20 G. Lammel; Cape, J. N. *Chem. Soc. Rev.*, 1996, **25**, 361.
21 B. J. Finlayson-Pitts; Wingen, L. M.; Sumner, A. L.; Syomin, D.; Ramazan, K. A. *Phys. Chem. Chem. Phys.*, 2003, **5**, 223 and references therein.
22 L. Gutzwiller; Arens, F.; Baltensperger, U.; Gäggeler, H. W.; Ammann, M. *Environ. Sci. Technol.*, 2002, **36**, 677.
23 Z. B. Alfassi; Huie, R. E.; Neta, P. *J. Phys. Chem.*, 1986, **90**, 4156.
24 L. Gutzwiller; George, C.; Rössler, E.; Ammann, M. *J. Phys. Chem. A*, 2002, **106**, 12045.
25 J. L. Miao; Wang, W. F.; Pan, J. X.; Lu, C. Y.; Li, R. Q.; Yao, S. D. *Radiation Phys. Chem.*, 2001, **60**, 163.
26 Z. Zhan; Yao, S.; Lin, W.; Wang, W. F.; Jin, Y.; Lin, N. *Free Rad. Res.*, 1998, **29**, 13.
27 F. Arens; Gutzwiller, L.; Gaggeler, H. W.; Ammann, M. *Phys. Chem. Chem. Phys.*, 2002, **4**, 3684.
28 R. Atkinson. *J. Phys. Chem. Ref. Data*, 1994, R1.
29 R. I. Olariu; Barnes, I.; Becker, K. H.; Klotz, B. *Int. J. Chem. Kin.*, 2000, **32**, 696.
30 W. F. Rogge; Hildemann, L. M.; Mazurek, M. A.; Cass, G. R.; Simoneit, B. R. T. *Environ. Sci. Technol.*, 1998, **32**, 13.
31 P. M. Fine; Cass, G. R.; Simoneit, B. R. T. *Environ. Sci. Technol.*, 2001, **35**, 2665.
32 C. Gallet; Keller, C. *Soil Biol. Biochem.*, 1999, **31**, 1151.
33 N. Lahoutifard; Ammann, M.; Gutzwiller, L.; Ervens, B.; George, C. *Atmos. Chem. Phys.*, 2002, **2**, 215.
34 M. Ammann; Rössler, E.; Strekowski, R.; George, C. *Phys. Chem Chem. Phys.*, 2004, **In preparation**.

35 X. Zhou; Beine, H. J.; Honrath, R. E.; Fuentes, J. D.; Simpson, W.; Shepson, P. B.; Bottenheim, J. W. *Geophys. Res. Lett.*, 2001, **28**, 4087.
36 X. Zhou; He, Y.; Huang, G.; Thornberry, T. D.; Carroll, M. A.; Bertman, S. B. *Geophys. Res. Lett.*, 2002, **29**, 26/1.
37 J. Kleffmann; Kurtenbach, R.; Lörzer, J.; Wiesen, P.; Kalthoff, N.; Vogel, B.; Vogel, H. *Atmos. Environ.*, 2003, **37**, 2949.
38 X. Zhou; Gao, H.; He, Y.; Huang, G.; Bertman, S. B.; Civerolo, K.; Schwab, J. *Geophys. Res. Lett.*, 2003, **30**, ASC 12/1.
39 K. A. Ramazan; Syomin, D.; Finlayson-Pitts, B. J. *Phys. Chem. Chem. Phys.*, 2004, **6**, 3836.
40 F. Rohrer; Bohn, B.; Brauers, T.; Brüning, D.; Johnen, J.-F.; Wahner, A.; Kleffmann, J. *Atmos. Chem. Phys. Discuss.*, 2004, **In press**.
41 E. R. Lovejoy; Huey, L. G.; Hanson, D. R. *J. Geophys. Res.*, 1995, **100**, 18775.
42 D. R. Hanson; Lovejoy, E. R. *J. Phys. Chem.*, 1996, **100**, 6397.
43 P. V. Danckwerts *Gas-Liquid Reactions*; McGraw-Hill: New York, 1970.
44 J. Heland; Kleffmann, J.; Kurtenbach, R.; Wiesen, P. *Environ. Sci. Technol.*, 2001, **35**, 3207.
45 J. Kleffmann; Heland, J.; Kurtenbach, R.; Lörzer, J. C.; Wiesen, P. *Environ. Sci. Pollut. Res.*, 2002, **9**, 48.
46 S. Trick. Formation of Nitrous Acid on Urban Surfaces - A Physical-Chemical Perspective, University of Heidelberg, 2004.
47 S. Inbar; Linschitz, H.; Cohen, S. G. *J. Am. Chem. Soc.*, 1981, **103**, 7323.
48 C. Murov S. L, I., Hug, G., L. *Handbook of Photochemistry*, 1993.
49 W. H. Melhuish. *J. Phys. Chem.*, 1961, **65**, 229.
50 C. A. Parker; Joyce, T. A. *Chem. Commun.*, 1966, 108.
51 P. K. Das; Bhattacharyya, S. N. *J. Phys. Chem.*, 1981, **85**, 1391.
52 P. K. Das; Encinas, M. V.; Scaiano, J. C. *J. Am. Chem. Soc.*, 1981, **103**, 4154.
53 S. Canonica; Jans, U.; Stemmler, K.; Hoigne, J. *Environ. Sci. Technol.*, 1995, **29**, 1822.
54 G. L. Squadrito; Fronczek, F. R.; Watkins, S. F.; Church, D. F.; Pryor, W. A. *J. Org. Chem.*, 1990, **55**, 4322.
55 G. Kaupp; Schmeyers, J. *J. Org. Chem.*, 1995, **60**, 5494.
56 T. A. Tuhkanen; Beltran, F. J. *Chemosphere*, 1995, **30**, 1463.
57 D. Vialaton; Richard, C.; Baglio, D.; Paya-Perez, A. B. *J. Photochem. Photobiol. A-Chem.*, 1999, **123**, 15.
58 S. Madronich. *J. Geophys. Res.-Atmos.*, 1987, **92**, 9740.
59 R. Atkinson; Baulch, D. L.; Cox, R. A.; Crowley, J. N.; Hampson, R. F.; Kerr, J. A.; Hynes, R. G.; Jenkin, M. E.; Rossi, M. J.; Troe, J. *IUPAC Subcomittee for Gas Kinetik Data Evaluation*, 2004, **Web-Edition**.
60 T. E. Graedel; Weschler, C. J. *Reviews Geophysical Space Physics*, 1981, **19**, 505.
61 S. Baraltosh; Chattopadhyay, S. K.; Das, P. K. *J. Phys. Chem.*, 1984, **88**, 1404.
62 S. Canonica; Hellrung, B.; Wirz, J. *J. Phys. Chem. A*, 2000, **104**, 1226.
63 A. A. Gorman; Rodgers, M. A. J. *J. Am. Chem. Soc.*, 1986, **108**, 5074.
64 C. Anastasio; Faust, B. C.; Rao, C. J. *Environ. Sci. Technol.*, 1997, **31**, 218.
65 T. Lögager; Sehested, K. *J. Phys. Chem.*, 1993, **97**, 10047.
66 J. K. Hurley; Linschitz, H.; Treinin, A. *J. Phys. Chem.*, 1988, **92**, 5151.
67 I. Loeff; Rabani, J.; Treinin, A.; Linschitz, H. *J. Am. Chem. Soc.*, 1993, **115**, 8933.
68 A. M. Grannas; Shepson, P. B.; Filley, T. R. *Glob. Biogeochem. Cycle*, 2004, **18**, art. no.
69 G. Mark; Korth, H.-G.; Schuchmann, H.-P.; von Sonntag, C. *J. Photochem. Photobiol., A*, 1996, **101**, 89.
70 H. J. Beine; Allegrini, I.; Sparapani, R.; Ianniello, A.; Valentini, F. *Atmos. Environ.*, 2001, **35**, 3645.

Table I Summary of the measured uptake coefficients on solid films using the coated wall flowtube /MS combination

Type	RH (%)	γ_{dark} (10^{-6})	γ_{light} (10^{-6})
Benzophenone		0.32	0.65
Benzophenone / Catechol		1.26	2.40
Benzophenone / Catechol	14	1.30	2.51
Benzophenone / Catechol	76	3.6	5.1
Catechol		0.07	1.4
Catechol	42	1.1	1.8
Anthracene		0.66	1.2
Anthracene	56	1.9	2.3
Catechol / Anthracene		< 0.1	0.89
Catechol / Anthracene	46	0.67	1.3
Anthrarobin	14	0.24	0.34

Table II. Reactivity and HONO-yields of the reaction of NO2 with differently composed organic films in the dark and under irradiation (300-420 nm)

type of organic coating and amount of organic compound used	% removal of initial [NO_2] by dark reaction[b] [%]	% yield of HONO per reacted NO_2 in dark reaction [%]	% removal of initial [NO_2] by light reaction[c,d] [%]	% yield of HONO per reacted NO_2 in light reaction [%]
sodium 4-benzoylbenzoate (1 mg)	4	7	20/17	45/48
4-benzoylbenzoic acid (1 mg)	2	n.a.	12/12	68/71
3,7-dihydroxy-2-napthoic acid (1 mg)	4	11	22/28/38[e]	67/74/77
perylene (0.5 mg)	3	n.a.	~0/0	n.a
syringic acid (1 mg)	6	6	7/7	36/43
3,4-dihydroxyphenylacetic acid (1 mg)	6	n.a.	1/2	n.a
potassium iodide (1 mg)	53	100	~0/0	n.a
external mixture[a]: sodium 4-benzoylbenzoate (1 mg) syringic acid (0.5 mg)	4	4	36/36	61/70
external mixture[a]: sodium 4-benzoylbenzoate (1 mg) 3,4-dihydroxyphenylacetic acid (1 mg)	2	n.a.	42/38	91/90
external mixture[a]: sodium 4-benzoylbenzoate (1 mg) potassium iodide (1 mg)	14	n.a	66/58	93/101
external mixture[a]: perilene (0.5 mg) 3,4-dihydroxyphenylacetic acid (1 mg)	2	n.a.	6/9	57/67
external mixture[a]: perilene (0.5 mg) potassium iodide (1 mg)	20	>80	7/10	n.a
internal mixture[a]: 4-benzoylbenzoic acid (1 mg) 3,4-dihydroxyphenylacetic acid (0.5 mg)	16	n.a	52/63	90/93
internal mixture[a]: 4-benzoylbenzoic acid (1 mg) 3,4-dihydroxyphenylacetic acid(1 mg)	7	n.a.	47/58	95/97

[a]The term external mixture is used when the reactor surface was coated first by the absorber molecule and subsequently by the phenol or potassium iodide. The term internal mixture is used when the reactor was coated from one solution containing both compounds.
[b]The removal of NO_2 due to the dark reaction was measured by exposing the coated wall reactor to the NO_2-mixture and measuring the decrease of the NO_2 concentration.
[c]The removal of NO_2 due to the light reaction was measured by illuminating the NO_2-mixture flowing through the coated wall reactor and comparing the NO_2 concentration before and during the irradiation.
[d]Values after 5 and 10 minutes of irradiation, respectively
[e]Values after 5,10 and 25 minutes of irradiation, respectively